European Journal of Molecular & Clinical Medicine
ISSN 2515-8260 Volume 07, Issue 07, 2020

In-vitro Antioxidant and Anticancer Evaluation of Newly Synthesized N-(5-oxo-2-phenylimidazolidin-1-yl)-4-(3,4-dihydroxyphenyl)-6-methyl-2-oxo-1,2,3,4-tetrahydropyrimidine-5-carboxamide

S. Shanmugam[1], Dr. K. Neelakandan[2], Dr. M. Gopalakrishnan[3], and Dr. S. Pazhamalai[4]

[1,3,4]Department of Chemistry, Annamalai University, Annamalainagar- 608 002, Tamilnadu, India

[2]Emcure Pharmaceuticals Limited, Pune – 411 057, Maharashtra, India

[4]E-mail: sripazhamalai@gmail.com ; [4]Mobile: +919047982112

Abstract: A novel *N*-(5-oxo-2-phenylimidazolidin-1-yl)-4-(3,4-dihydroxyphenyl)-6-methyl-2-oxo-1,2,3,4-tetrahydropyrimidine-5-carboxamide (**1)** was synthesized using Biginelli reaction at room temperature. The dual heterocyclic compound 1 was characterized using the analytical techniques such as FT-IR, ^{1}H & ^{13}C-NMR, Mass analysis, UV-visible and fluorescent spectroscopic system. The data on charge density was used to explain the characteristics of molecular systems. In addition, in the form of the complete and partial density of states, the HOMO-LUMO energy gap, electrostatic potential map and some quantum chemical insights have been obtained. Furthermore, to demonstrate the possible applications of dihydropyrimidinone **1** in nonlinear optics the polarizability and first hyperpolarizability were measured. Molecular docking is also determined in order to illustrate the overexpression of estrogen receptor in 80 % of 2J9M protein. The compound **1** was subjected for its antioxidant (ABTS) and anticancer activity (DPPH) by *in-vitro* analyses and found with substantial antioxidant activity.

Keywords: Biginelli reaction, Dihydropyrimidinone, anticancer, antioxidant, DPPH & ABTS method, HOMO-LUMO, and NLO.

1. INTRODUCTION

Novel and efficient synthesis of substituted pyrimidine and many detailed reviews have been appeared. [1-8] In medicinal chemistry, the pyrimidine nucleus is a major pharmacophore. The primary goal of current drug research remains the synthesis of novel pyrimidine derivatives for further production of better therapeutic agents. The versatility of newer generation pyrimidines will constitute as a fruitful pharmacophore. Researchers have since been drawn to the production of more potent pyrimidine derivatives with a large spectrum of biological activity. [9] The pyrimidine ring a core of uric acid, purine, alloxan and barbituric acid is also combination of some antibacterial and anti-malarial agents. As an essential part of DNA and RNA, pyrimidine imparts different pharmacological properties, such as effective bactericides and fungicides. [10,11] Certain pyrimidine derivatives are also known to possess anticonvulsant [12] antifilarial, [13] antifungal, antibacterial, [14,15] antihistamine [16] and antimalarial [17] activities. Several antihypertensive agents, calcium channel blockers, adrenergic, and neuropeptide antagonists have appeared as integral backbones of some of the 3,4-dihydropyrimidines.[18] In the literature with intriguing biological activities such as anti-HIV natural product (alkaloid) batzelladine B and some natural marine products containing 3,4-dihydropyrimidine core have also been identified. [19,20]

In line with the above continued efforts in synthesize of bioactive lead compounds for health care, the title compound has been designed using a key intermediate Biginelli reaction product viz., ethyl 4-(3,4-dihydro-xyphenyl)-6-methyl-2-oxo-1,2,3,4-tetrahydropyrimidine-5-carboxylate. The Biginelli reaction product was synthesized by reacting multicomponent such as urea, ethyl acetoacetate and 3,4-dihydroxy benzaldehyde in ethanol in the presence of catalytic quantity of conc. hydrochloric acid. Reaction of ethyl 4-(3,4-dihydroxyphenyl)-6-methyl-2-oxo-1,2,3,4-tetrahydropyrimidine-5-carboxylate with hydrazine hydrate resulted 4-(3,4-dihydroxy-phenyl)-6-methyl-2-oxo-1,2,3,4-tetrahydropyrimidine-5-carbohydrazide (Carbohydrazide). Condensation of the carbohydrazide with benzaldehyde yielded *E-N*'-benzylidene-4-(3,4-dihydroxyphenyl)-6-methyl-2-oxo-1,2,3,4-tetrahydropyrimidine-5-carbohydrazide (Schiff base). The Schiff bases thus produced were cyclized by condensation with glycine to imidazolidinone in benzene and ethanol. Based on the physicochemical and FT-IR, ^{1}H & ^{13}C-NMR, Mass, UV-visible and fluorescent spectral data, the structure synthesized compound was elucidated. The anticancer efficacy of the compound **1** against the MCF-7 cell line was studied through the in-vitro anticancer exploration. The broad spectrum of antioxidant activity was also studied with the comparison with a standard.

Experimental

2. MATERIALS AND METHODS

All the chemicals are purchased from Sigma-Aldrich (India). Toluene: ethyl acetate (1:9) was the solvent mixture used for the TLC analyses. Iodine vapor staining technique was used in analyzing the TLC spots. Melting points were determined in open-end capillary method. Elemental analysis is conducted using a Thermo Scientific (FLASH 2000) Elemental Analyzer. FT-IR spectra was recorded between 400-4000 cm^{-1} on a Nicolet Avatar 330 FT-IR spectrometer using KBr pellet technique. Using DMSO-d_6 as standard, ^{1}H & ^{13}C-NMR was registered on a Bruker 400 MHz spectrometer. Chemical shifts were recorded in parts per million (ppm). ESI-Mass spectrum is measured in positive and negative mode on a SCIEX-API 2000 ESI-MS spectrometer for the synthesized compound. UV-Vis and fluorescence measurement was performed using the Perkin-Elmer LS45 fluorescence spectrophotometer with a scan rate of 1200 nm at room temperature.

Synthesis of Biginelli compound

A mixture of 0.15 mole of urea (CH_4N_2O), 0.1 mole of ethyl acetoacetate ($C_6H_{10}O_3$), and 0.1 mole of 3,4-dihydroxybenzaldehyde ($C_7H_8O_3$) was dissolved in 25 mL of C_2H_5OH along with 2 drops of conc. HCl and refluxed for 4 h. The reaction mass was poured in a beaker containing 100 mL ice-cold H_2O with stirring and left overnight at room temperature. Next day, the solid was filtered, washed with water and dried. The solid was recrystallized from C_2H_5OH. The purity of the compound was determined by thin-layer chromatography.

Synthesis of carbohydrazide

A mixture of 0.1 mole of Biginelli compound and 0.1 mole of hydrazine (N_2H_4) was dissolved in 20 mL of C_2H_5OH along with 2 drops of conc. H_2SO_4 and refluxed for 3 h. The solvent from the reaction mixture was evaporated to obtain a residue. The residue was dissolved and recrystallized from C_2H_5OH. Recrystallized compound's purity was assessed by thin-layer chromatography.

Synthesis of Schiff bases of dihydropyrimidinone

About 0.01 mole of carbohydrazide and 0.01 mole of benzaldehyde were dissolved in C_2H_5OH. 5 mL of glacial CH_3COOH was added and the content was refluxed for 4 h. The reaction mixture was then poured in a beaker containing ice-cold H_2O. The precipitated product was filtered,

washed with water and dried. The precipitate was then recrystallized from C_2H_5OH. The purity of the compound was assessed using thin-layer chromatography.

Synthesis of dihydropyrimidinone

A mixture of 0.01 mole of Schiff base and 0.01 mol of Glycine ($C_2H_5NO_2$) in C_2H_5OH was refluxed for about 4 h. After cooling, the mixture was poured in a beaker containing ice-cold H_2O. The precipitated product was filtered, washed with water and dried to afford the title compound. The precipitate was then recrystallized from C_2H_5OH. The purity of the compound was determined using thin-layer chromatography.

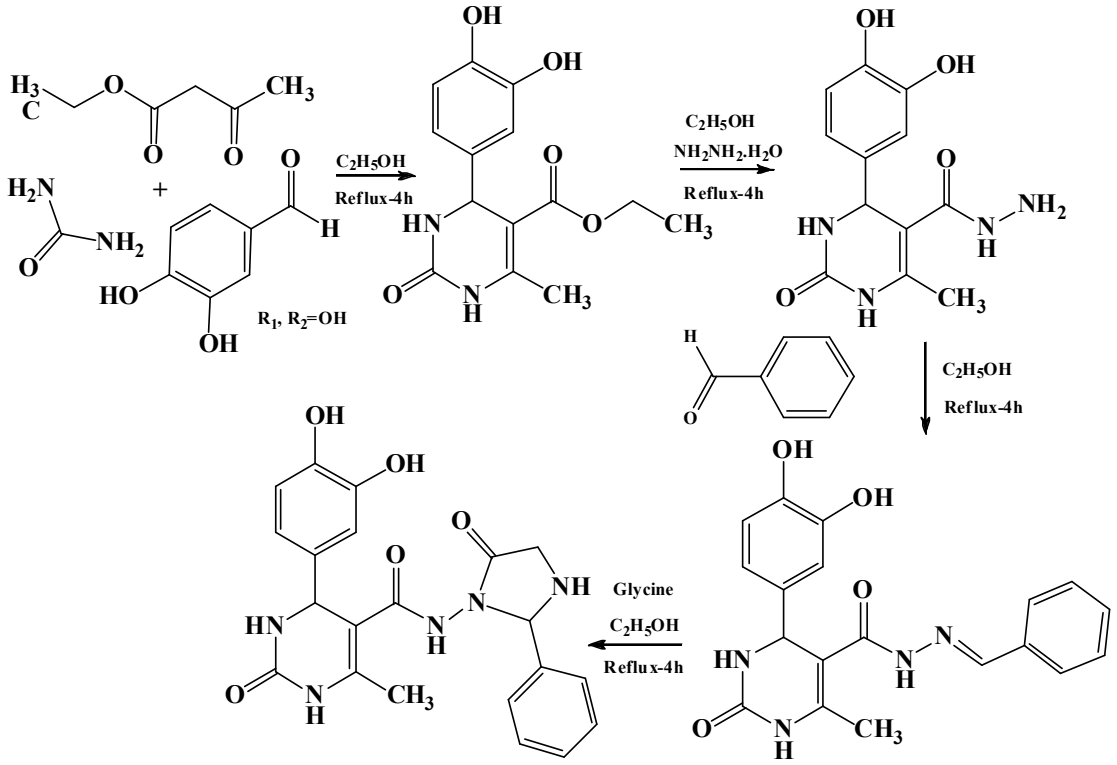

Scheme 1. Synthesis of compound **1**

N-(5-oxo-2-phenylimidazolidin-1-yl)-4-(3,4-dihydroxyphenyl)-6-methyl-2-oxo-1,2,3,4-tetrahydropyrimidine-5-carboxamide (1)

Yield: 77 %. Melting point: 206-210°C; Chemical Formula: $C_{21}H_{21}N_5O_5$; Calculated %: C, 59.57; H, 5.00; N, 16.54; Found %: C, 59.51; H, 5.03; N, 16.50; FT-IR (KBr) cm^{-1}: 3412.40 (O-H stretching, Phenol), 3307.08 (2° N-H stretching, amides), 3051.02 (sp^2 C-H stretching, aromatics), 2924.15 (sp^3 C-H stretching, alkanes), 1609.01 (C=O stretching, amides), 1459.39 (C-H bending, CH_2 group), 1356.12 (C-H bending, CH_3 group), 1231.37 (C-O-H stretching, Phenol), 1144.66 (C-O stretching, Phenol). ^1H NMR (DMSOd_6, 400 MHz, δ): 9.124 (s, 1H, OH), 8.880 (s, 1H, OH), 8.718 (s,1H, NH), 7.641 (s,1H, O=CNH), 1.123 (s, 3H, CH_3), 6.605-6.801 (m, 12H, Ar-H), 4.012 (s,1H, CH_2). ^{13}C NMR (DMSO-d_6, 400 MHz, δ): 146.33 (C-OH), 148.45 (C=O), 14.70 (CH3), 147.80 (C-CH3), 166.02 (O=C-NH), 54.10 (CH_2 of imidazolidinone ring), 136.46 (C-phenyl ring), 115.82 (2CH), 118.83 (2CH). ESI-MS: Calculated: m/z = 423.15; Found: m/z = 424.33 [M ± 1] ion.

Computational details

The density functional theory calculation for the new compound **1** is done using Gaussian 03W software at B3LYP/6-31G (d,p) level. The frontier molecular atomic orbital is also analyzed on the fundamental of the HOMO-LUMO energy gap. The Mulliken atomic charges, dipole moment, polarizability, hyperpolarizability, geometrical parameters are determined.

Molecular docking Procedure

Protein preparation

Molecular docking simulation is conducted on the dihydropyrimidinone compound 1 structure and 3D structure-based pharmacophore models are used to classify the molecular interactions of alpha-mangostin and its estrogen receptor alpha (ER_a) derivatives (PDB ID: 2J9 M) are collected from the Brook-haven Protein Data Bank (RCSB) (http:/www.rcsb.org/pdb). Using the protein preparation wizard, the protein was pre-processed and packaged. Using a Scan and Alter panel, the unnecessary protein chains and water molecules are eliminated. In order to minimize the complex, the OPLS-2005 force field is used. The grid is generated and imported into GLIDE Docking using the generation panel of the receptor grid.

Ligand Preparation

The molecular structure of Receptor 1 is drawn using Chem Office 8.0 and stored in the SDF file format. The structure file of dihydropyrimidinone compound 1 is imported into project table Maestro and reduced using the force field of OPLS 2005 (Optimized Potential for Liquid Stimulation). To neutralize the compound charge and ionization, the EPIK program is used.

Molecular Docking

The ligands and proteins prepared in silico are used with Glide for molecular docking. Extra Precession (XP docking) is used to classify the protein-ligand interaction.

Cell culture

The MCF-7 cell line (NCCS, Pune, India) is grown with 10 percent FBS and antibiotics (penicillin-100 µg / mL; streptomycin-50 µg / mL) supplemented with DMEM. In 95% air, 5% CO_2 incubator, cells are cultured at 37ºC.

Anticancer activity, Cell viability assay

Dihydropyrimidinone compound cytotoxicity was tested against MCF-7 cell lines using the 3-(4,5-dimethylthiazole-2-yl)-2,5-diphenyltetrazolium bromide (MTT) assay. At a density of 1.5×10^4 cells per well, the cells are seeded into a medium containing a 96-well plate and incubated in dihydropyrimidinone compound at a concentration ranging from 0.9 to 500 µM for 48 hours. For each treatment, triplicate wells were maintained, with 100 µL of MTT per well. To allow MTT to form formazan crystals by reacting with MTT and metabolically active cells, it is incubated at 37ºC for 4 hrs. The medium with MTT is carefully discarded from the wells. Every well is applied to dissolve intracellular formazan crystals with 100 µL of DMSO, and the plates are shaken for 10 min. Absorption is read out at 350-500 nm using ELISA (enzyme-linked immunosorbent assay) readers. Using a fluorescence microscope, the cell photos are analyzed. The proportion of survival is calculated using the formula:

$$\% \text{ survival} = [\text{live cell number (test)}/\text{live cell number (control)}] \times 100$$

DPPH radical scavenging assay

According to the Blois process, the DPPH assay was carried out. The reaction is based on the reduction of a stable free radical called 1,1-diphenyl-2-picrylhydrazyl (DPPH). This gives rise to a reduced form with the lack of pale violet color when DPPH reacts with a product that can donate a nitrogen atom; pale yellow colors remain from the phenyl group. The antioxidant activity of the compound, using the DPPH process, was calculated in terms of radical scavenging capacity. Different sample concentrations (20, 40, 60, 80, 100µg / mL) and reference compounds of ascorbic acid were prepared in an ethanol solution of 0.3mM of DPPH. The mixture was violently shaken and allowed to stand for 30 minutes in the dark at room temperature. Then, at 350-500 nm against a blank, the absorbance was assessed. The inhibition percentage was determined by comparing the absorption values of the control samples and the test samples. The percentage of inhibition was calculated using the following equation:

$$\text{Percentage inhibition (I \%)} = (A_{control} - A_{sample} / A_{control}) \text{ X } 100$$

Where '$A_{control}$' was the absorbance of the control and 'A_{sample}' was the absorbance of the sample. The antioxidant activity of the compound was expressed as IC_{50}. (IC_{50} - concentration required to obtain a 50% radical scavenging activity). Ascorbic acid was used as the positive control.

ABTS Radical Scavenging Assay

The radical scavenging behavior of ABTS was calculated by Re method-azinobis(3-ethylbenzo thiazoline-6-sulfonic acid) (ABTS) radical cation (ABTS*+) was formed by reacting at room temperature at equivalent amounts of 7 mM ABTS salt and 2.45 mM ammonium persulfate and the mixture was allowed to stand at room temperature for 16 hours in the dark. The samples were allowed to react at different concentrations (20, 40, 60, 80, 100µg / mL) with 900 µL of ABTS solution. The absorbance reading was registered at 350-500 nm after 20 minutes and was compared with the power. The experiments were all carried out in triplicate. The proportion of ABTS+ inhibition by the sample was determined as follows:

$$\text{Percentage inhibition (I \%)} = (\text{A control- A sample /A control}) \text{ X } 100$$

3. RESULTS AND DISCUSSION

Chemistry

In a four-step process, the title compound 1 was synthesized. The first step was the synthesis of dihydropyrimidinone in the presence of acid and ethanol, widely known as the Biginelli reaction, by the condensation of urea with ethyl acetoacetate and 3,4-dihydroxy benzaldehyde. The advantage is that it is a convenient intermediate to have a heterocyclic compound that is medically essential. In order to have carbohydrazide, dihydropyrimidinone was further condensed with hydrazine hydrate. Finally, the dihydropyrimidine carbohydrazide was condensed with aldehyde to yield the Schiff bases, which were further cyclized to give the desired compound with glycine in the presence of benzene and ethanol. The melting point of the title compound was reported. The melting point was determined in open capillary tubes with an electrically heating melting point apparatus and is uncorrected. The solubility of the synthesized compound was checked by using the following solvent: DMSO. Thin-layer chromatography with silica gel as a stationary phase, toluene: ethyl acetate (1:9) as the mobile phase was used to test the purity of the title compound, visualizing spots using iodine vapors. The synthesized compound's infrared spectrum was recorded and represented in cm^{-1} (wavenumber). The synthesized compound's NMR spectrum had been recorded

and interpreted, to confirm the imidazolidinone ring formation (the presence of CH_2 proton). Mass spectral data were also found to be consistent with the predicted structure. A spectrum of UV-Vis / Fluorescence was used to identify the compound. The characterized compound **1** is obtained with a good yield. The general chemical reaction is pictured in **Scheme 1**. The synthesized compound exhibited pronounced molecular docking, anticancer activity, antioxidant activity and DFT study.

Experimental spectroscopic properties of compound 1

The redshift of absorption and emission is usually directly proportional to the transition of charge within the compound. This is based on the conjugation within the molecule in a donor-π-acceptor structure. In our analysis, we observed a propensity for compound 1 to show redshift, compound 1 to show absorption at 357 nm and chloroform emissions at 403 and 490 nm, absorption at 350 nm, and methanol emissions at 400 and 495 nm. **Table I** display the full photophysical properties of compound **1** and is shown in **Fig 1** and **Fig 2** for chloroform & methanol, which have different polarities in two different solvents. Compound 1 has a marginal change in the overall absorption and the maximum emission steadily changed to the red side of the UV-visible spectrum with the rise in solvent polarity.

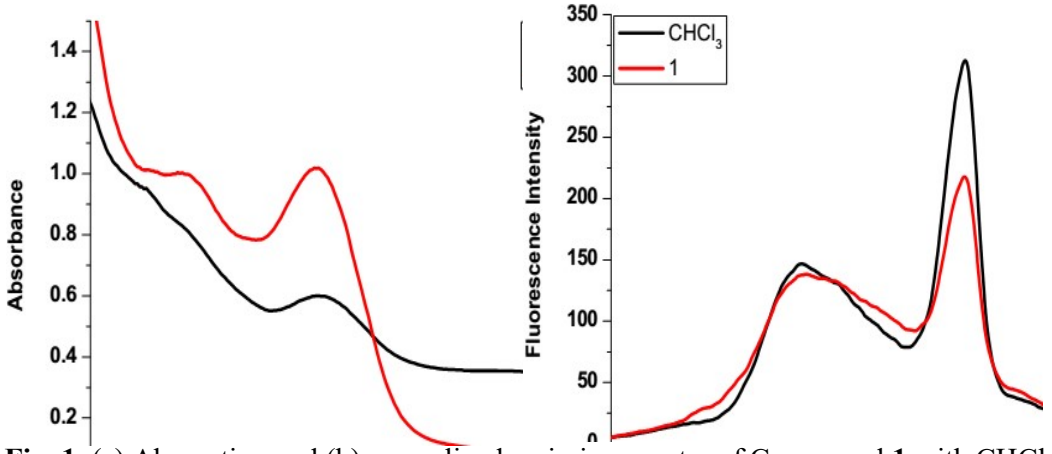

Fig. 1. (a) Absorption and (b) normalized emission spectra of Compound **1** with $CHCl_3$

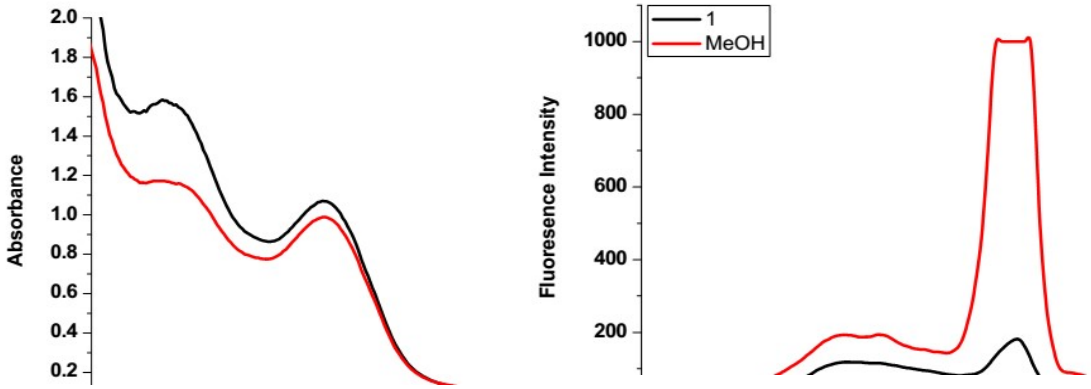

Fig. 2. (a) Absorption and (b) normalized emission spectra of compound **1** with MeOH

Table I - Absorption and emission properties of compound **1**

Compound	Solvent	λ^{a}_{max} nm	λ^{b}_{max} cm^{-1}	ε^{c}	λ^{d}_{max} nm	λ^{e}_{max} cm^{-1}	$\Delta^{f}\nu$ cm^{-1}
1	$CHCl_3$	357	2.73	3.95	403 & 490	13188.73	7982.10
	MeOH	350	2.66	3.89	400 & 495	13179.80	7950.03

Computational studies of compound 1

The DFT computation is done at the B3LYP/6-31G basis set level on a private computer using a Gaussian 03W program package. The optimized molecular geometry structure is shown in **Fig 3**.

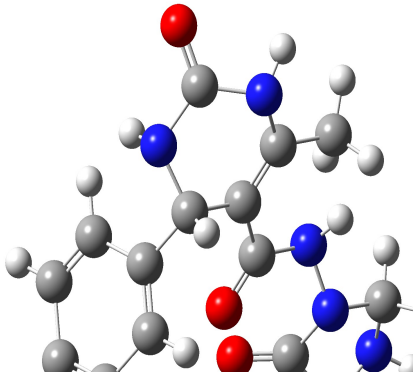

Fig. 3 Optimized structures of compound **1**

Molecular geometry

The geometry optimization of Dihydropyrimidinone **1** was determined at B3LYP level theory with a 6-311 + G(d,p) basis set and accordance with the atom numbering scheme of the molecule shown in **Fig. 4**.

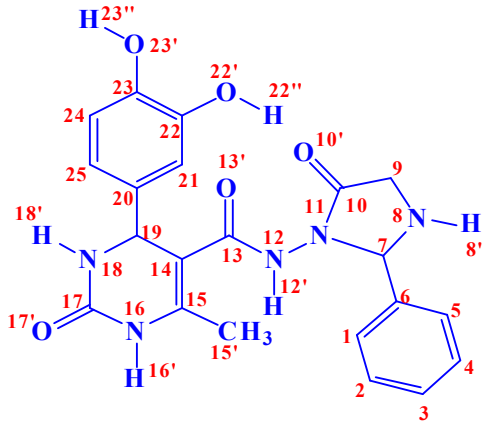

Fig. 4 Numbering pattern of compound **1**

FMO analysis

The energy of HOMO and LUMO determines how the molecule interacts with other species and helps to explain the molecule's chemical reactivity and kinetic stability. From the energy difference (ΔE), the electronic and optical properties of the molecule can be obtained. HOMO has the capacity to give electrons, and LUMO has the capacity to accept electrons. The space distance of the HOMO-LUMO is the potential energy difference between the HOMO-LUMO orbitals shown in **Fig 5**. Basically, it gives the molecule how much energy needs to be fed into it to kick it into an excited state from the ground state (the most stable). The energy separation value between HOMO and LUMO in gas is 3.87eV, respectively. The limited energy gap obtained is also an indication that the complex can be readily polarized and interactions within the compound occur through molecular charge-transfer. In comparison, the growing importance of the energy difference indicates that the molecule becomes more stable when moving from the solution to the gas phase. **Table II** on the basis of the expected energy values (eV) of compound dihydropyrimidinone 1 in gas phase values, and thus the polarity of the solvent determines the dipole moment of the molecule. Based on Koopman's theorem, the chemical reactivity and site selectivity of molecular systems have been determined.

Table II - Calculated energy values (eV) of compound **1** in the gas phase

B3LYP/6-311++G(d,p)	**1**
E_{HOMO}	-5.35
E_{LUOMO}	-1.48
$E_{LUMO-HOMO}$	3.87
Electronegativity	-3.42
Hardness	1.93
Electrophilicity index	3.07
Softness	7.03

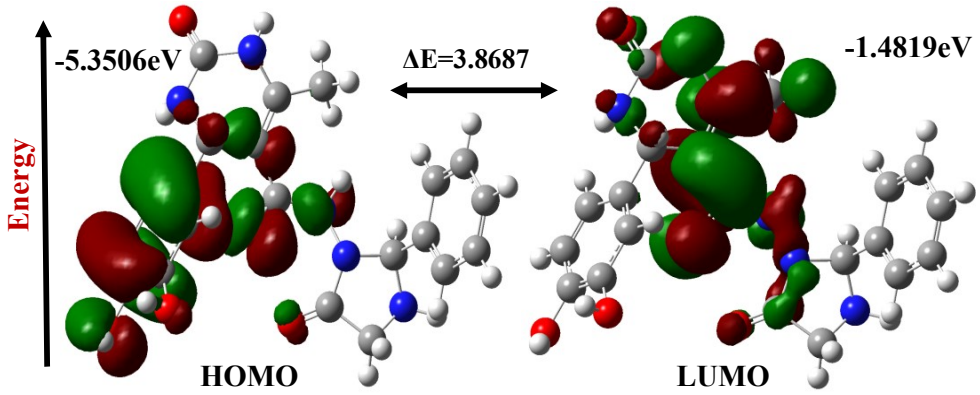

Fig. 5 HOMO and LUMO molecular orbitals in the gas phase of compound **1**

Chemical hardness is related to the stability and reactivity of chemical compounds and measures resistance to changes in the distribution of electrons or the movement of charges. Chemical hardness refers, from this point of view to the difference between HOMO and LUMO. The wider the energy difference between HOMO and LUMO, the molecule is harder and more stable / less reactive. The higher value of ΔE reflects a compound with greater hardness or less softness. The electron-acceptance ability of the systems is relatively close to chemical potential and hardness, defined by another global reactivity descriptor electrophilicity index (ψ). High electrophilicity index values improve the molecules' electron-acceptance capacity.

Mulliken atomic charge analysis

A molecule bonding potential relies on the electric charge on the atoms. The Mulliken and natural population analysis derived the atomic charge values. By calculating the electron population of each atom as described by the 6-31 G (d, p) basis set, Mulliken and natural charge distributions were determined. In **Table III**, the measured charge values are tabulated. The schematic shapes of our observations are seen in **Fig 6**. Positive and negative are found to be the magnitude of the carbon atomic charge. Owing to its attachment to the electronegative oxygen atom, all the charges of the carbon atoms bound to the electronegative atoms are positive. These electronegative atoms took out the carbon atom partial charges and thereby became positive.

Table III - Mulliken atomic charges of compound **1**

Atom	**1**	**Atom**	**1**	**Atom**	**1**
C-1	-0.104	N-12	-0.320	C-19	0.031
C-2	-0.101	H-12’	0.267	C-20	-0.111
C-3	-0.093	C-13	0.445	C-21	0.001
C-4	-0.098	C-13’	-0.313	C-22	0.105
C-5	-0.081	C-14	-0.201	O-22’	-0.421
C-6	-0.004	C-15	0.153	H-22”	0.247
C-7	0.026	C-15’	-0.351	C-23	0.180
N-8	-0.403	N-16	-0.375	O-23’	-0.397
H-8’	0.205	H-16’	0.221	H-23”	0.238
C-9	-0.062	C-17	0.400	C-24	-0.075
C-10	0.310	O-17’	-0.360	C-25	-0.067
C-10’	-0.283	N-18	-0.339		
N-11	-0.276	H-18’	0.218		

The magnitude of the atomic charges for the title compound is found to be highly positive for H8’, C10, H12’, C13, C15, H16’, C17, H18’, C22, H22”, C23 and H23’’. The maximum negative values observed in N8, C10’, N11, N12, C13’, C14, C15’, O17, N18’, C20 and O22’. O23”. From these studies, the high negative charge and positive charge at O22’ and C13 suggest that charge delocalization occurs in the entire molecule shown in **Table III**.

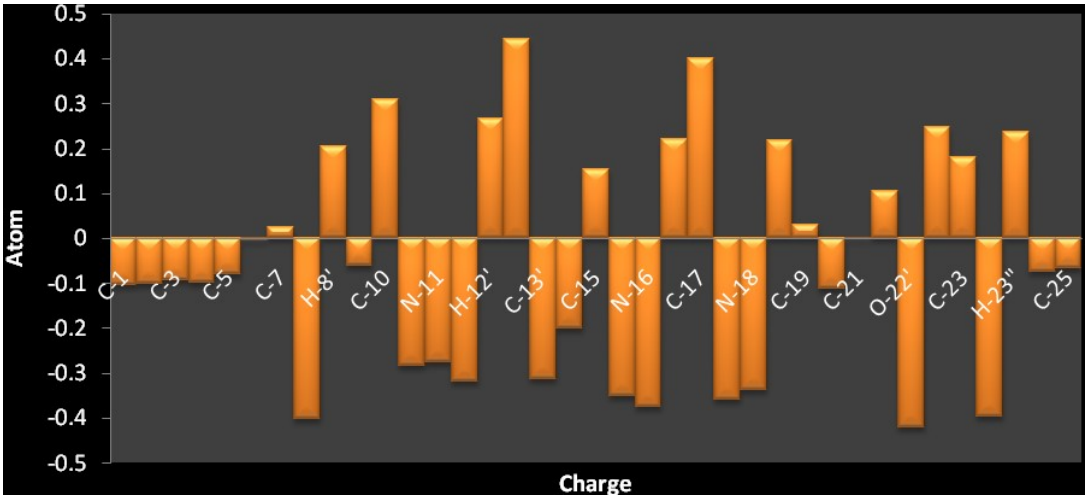

Fig 6. Mulliken atomic charge distribution of compound **1**

Nonlinear optical effects

In the fields of telecommunications, signal processing, propagation of optical signals, optical interconnection, imaging, laser and other optoelectronic uses, organic and inorganic materials with NLO characteristics have been used. Organic materials are of considerable significance among the materials producing NLO effects because of their synthetic durability, ultra-fast reaction times, large hyperpolarizability, and high thresholds of laser damage compared with inorganic materials. Organic molecules often have donor-acceptor groups bound to an aromatic ring structure that enhances the transfer of charge by delocalization of π-electrons. Reliable estimates are given by theoretical calculations based on quantum mechanics which allow the determination of the magnitude of the dipole moment, polarizability, and hyperpolarizability of the substance to help us determine the character of the NLO.

Table IV - Dipole moment, the polarizability of compound **1**

Parameter	Dipole moment (Debye)
	1
μ_x	7.3134
μ_y	0.9955
μ_z	2.1811
μ_{total}	7.6963
Parameter	Polarizability (a.u)
α_{xx}	166.87
α_{yy}	193.70
α_{zz}	175.55
α_{xy}	13.29
α_{xz}	6.62
α_{yz}	12.59
α_o (esu)x10^{-23}	2.65
$\Delta\alpha$ (esu) x10^{-24}	5.5

The NLO property of the title compound is, thus, greater than urea. Data provided in **Table IV** and **Table V** indicate that the title compound is 1 (HF) times greater than urea. The numerical values of the dipole moment, polarizability, first-order hyperpolarizability, are considered to provide an understanding of the compound's NLO character.

Table V - Hyperpolarizability values of compound **1**

Parameter	Hyperpolarizability (a.u)
	1
β_{xxx}	69.5183
β_{yyy}	-117.72
β_{zzz}	41.3235
β_{xyy}	135.222
β_{xxy}	-106.23
β_{xxz}	83.2436
β_{xzz}	-44.127
β_{yzz}	-19.789
β_{yyz}	17.7611
β_{xyz}	48.6292
β_0 (esu) $x10^{-30}$	2.8

Docking analysis of compound 1

The Dihydropyrimidinone scaffold has helped us to build and develop methods for identifying a new drug. While small molecules (substrate, inhibitor, drug, or drug candidate) and the target macromolecule (receptor, enzyme, or nucleic acid) match together, molecular docking is carried out on gauge valuate. This can be beneficial for the development of improved medicines and also for the understanding of the nature and degree of the receptor binding of molecules. Molecular docking tests are then carried out to elucidate that a particular protein tyrosine kinase (PDB: 2J9 M) is identified because of the target for cytotoxicity compounds in silico antioxidant studies. Their PDB file is retrieved from the protein database and used until all little water, cofactors, and ligands are extracted. Compound 1 showed a layout value of -8.147 kcal/mol of glide energy. The ligand was docked with the crystal structure of the complex with Macrocyclic Aminopyrimidine (PDB ID: 2J9 M) along with a test compound from the Protein Data Bank in an effort to understand the binding mode of compound 1 (**Fig . 7**). Compound 1 best scoring pose from the docking experiments is seen in **Fig . 7** along with receptor residues that interact inside binding sites with the ligand.

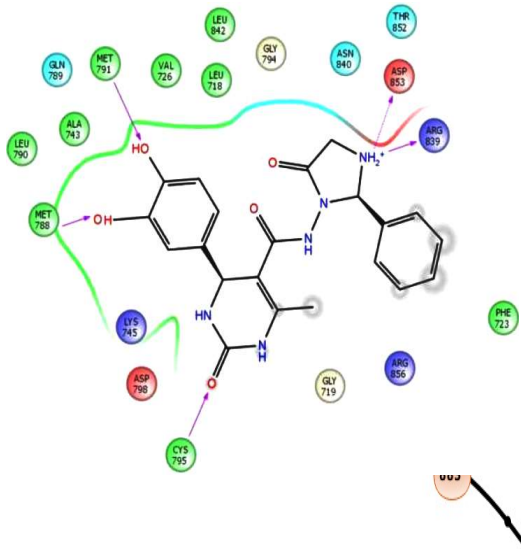

Fig 7. Molecular docking study of PDB code: 2J9M with the various non-covalent interactions of compound-1/2d images.

As detected by glide molecular docking, the lowest binding energy for the ligand-ER (PDB ID: 2J9 M) protein interaction showed that compound 1 had the highest G scores (-9,006 kcal mol-1 respectively). From the docking tests, we find that most of the ligands form hydrogen bonds with the surrounding hydrophobic residues MET788, ASP853, ARG839, LYS745, CRY794, and GLU789 in the Helix 12 through the amide groups with four residues (LYS1053, SO4302) and van der Waals (vdW) interactions. In addition, for the active interaction of the compound with the receptor, the keto group is also necessary (**Table VI**).

Table VI - Molecular Docking Studies of compound **1**

Comp.	glide gscore	glide evdw	glide ecoul	glide energy	Interacting Residues
1	-8.147	-47.228	-6.829	-49.995	MET788, ASP853, ARG839, LYS745, CRY794, GLU789
Regorafenib	-9.006	-43.643	-7.074	-50.717	LYS1053, SO4302
glide evdw = van der Waals interaction energies, glide ecoul = Coulomb interaction energies					

Prediction of Pharmacokinetic Properties

The 2D compound 1 structure was subjected to a computer programme using the Schrödinger software Qikprop package for the in-silico determination of pharmacokinetic properties. The statistical parameter of compound 1 pharmacokinetic property was seen in **Table VII** and **Table VIII**. Compound 1 estimate of pharmacokinetic properties suggest that the compound was endowed with drug-like properties. The findings showed that in accordance with the law of five, there is one infringement. Compounds have a molecular weight ranging from 423.15 to 482.82 amu. The number of donors of hydrogen bonds is 0, while the values of acceptors of hydrogen bonds range from 7 to 6. Furthermore, the values of the partition coefficient of all substances are less than seven.

Table VII - Lipinski's rule of five factors of compound **1**

Comp.	**Factors of Lipinski's rule of five**				
	mol_MW (<500)	**Donor HB (< 5)**	**Accpt HB (< 10)**	**QPlogPo/w (< 5)**	**Rule of Five**
1	423.15	4	7	3.571	0
Regorafenib	482.82	3	6	4.209	0

The compound tested has a cumulative percentage of less than 100% human oral absorption compound. There are permissible criteria for the aqueous solubility (QPlogS) parameter and the HERG K+ channel block (QPlog HERG) IC_{50} value of the measured compound. The blood-brain barrier permeability prediction (QPlogBB) for the studied compound was calculated and appropriate values were predicted to range from -1.12 to -0.98.

Table VIII - Pharmacokinetic Properties of compound **1**

Comp.	**Pharmacokinetic properties**			
	Percent Human Oral Absorptiona (> 100 high, < 25 poor)	**QPlogSb (–6.5 to 0.5)**	**QPlogHERGc (below –5)**	**QPlogBBd**
1	95.35	-5.116	-4.913	-1.12
Regorafenib	94.23	-7.224	-5.511	-0.98
[a] Percentage of human absorption, [b] Predicted aqueous solubility; S in mol/L, [c] Predicted IC_{50} value for the blockage of HERG K+ channels, [d] Predicted blood-brain barrier permeability.				

Cytotoxicity

The compound 1 cytotoxicity responses of varying concentrations were studied. This is apparent from the cellular imaging process. This finding is thus an important candidate for observing changes in intracellular concentration under certain biological conditions within compound 1 and has justified its cytotoxicity, MTT assay, in cancer cells of MCF-7. The effects of newly synthesized materials on MCF-7 cancer cell proliferation inhibition have been assessed by the MTT assay.

Briefly, the cells ($1X10^4$) were inserted well after harvesting and allowed to stick for 24 hours. Then the synthesized substance in each well was treated with 100 µL of varying concentrations (ranging from 0-500 µM concentration). 100 µL of MTT was applied after 24 h of treatment and incubation was prolonged for another 4 h, **Fig 8**.

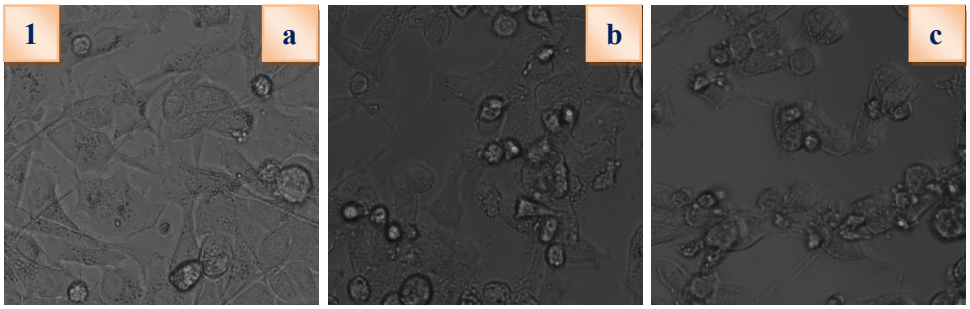

Fig. 8. Live-cell image of compound **1**: (a) before and (b and c) after treatment with compound **1** examined by fluorescence microscopy.

Live-cell images of compound 1: (a) before and (b and c) during fluorescence microscopy of compound 1 treatment. Then, by adding 100 µL DMSO a quantity, the reaction was stopped and tested (350-500 nm). As concentration reduces cancer cell development by 50% (IC_{50}), cytotoxicity has been suggested. Synthesized compound IC_{50} value (**Fig 9**) and compound 1 demonstrated maximal cell death in cancer cells (35.78 µM). The corresponding IC_{50} values for compound 1 against MCF-7 cell lines are seen in **Table IX**.

Table IX - The IC_{50} values of compound **1** against MCF7 cell lines.

Anticancer effect of compound 1 on MCF7 cell line	
Concentration (µM)	**Cell Viability %**
	1
0	100
0.9	74.51
1.9	64.45
3.9	55.65
7.8	41.17
15.6	34.48
31.25	23.55
62.5	17.42
125	11.81
250	6.66
500	2.33

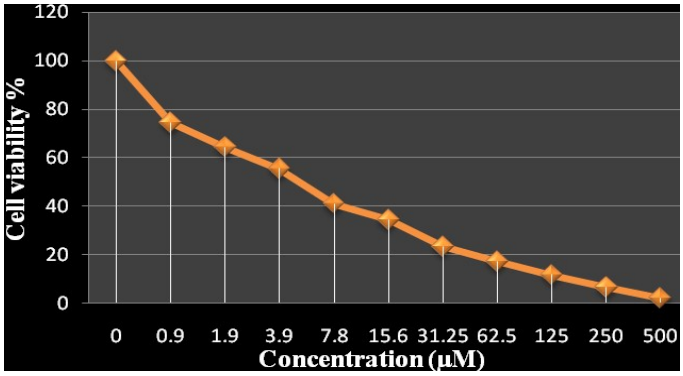

Fig. 9 The IC_{50} values of compound **1** against MCF7 cell lines.

Antioxidant Activity

The compound was also evaluated by DPPH and ABTS for in vitro antioxidant evaluation and its free radical scavenging property was recorded.

DPPH radical scavenging assay

The synthesized compound showed interesting antioxidant activity compared to standard. Among them, compound 1 was found to be more potent with an IC_{50} value of 73.03 µM respectively, comparable to standard with IC_{50} values 42.75 µM.

The presence of hydroxy group on the phenyl ring of the imidazolidinone ring showed promising activity. Replacement of electron releasing groups on phenyl ring linked to both the moieties showed moderate activity Presence of oxygen atom at the 2nd position of dihydropyrimidinone ring has improved antioxidant effect. The percentage inhibition values and IC_{50} values are tabulated in **Table X** and illustrated in **Fig. 10.**

Table X - The DPPH radical scavenging activity of the synthesized compound **1**

Antioxidant effect of compound 1		
Concentration (µg/mL)	**% Inhibition**	
	1	**Standard**
20	18.07 ± 0.50	22.99 ± 0.71
40	21.18 ± 0.16	42.02 ± 0.18
60	33.24 ± 0.29	55.23 ± 0.49
80	49.19 ± 0.84	93.20 ± 0.52
100	72.12 ± 0.29	110.02 ± 0.73
IC_{50}(µM)	73.03	42.75

Each value is expressed as a percentage of activity mean ± standard deviation (n = 3)

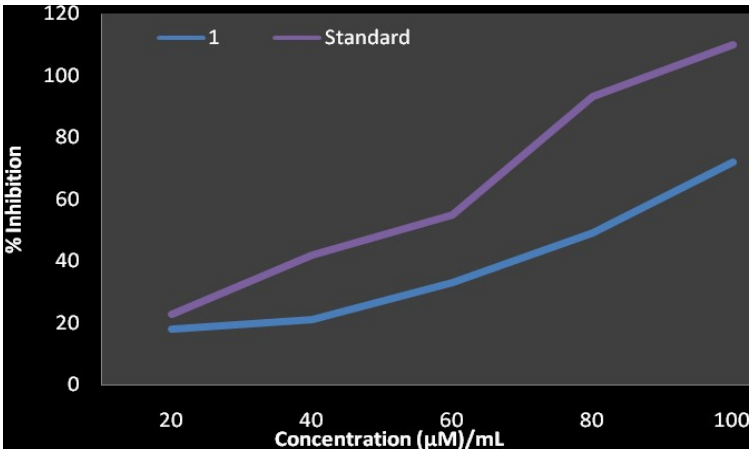

Fig. 10 *Invitro* antioxidant activity by DPPH method of compound **1**

ABTS Radical Scavenging Assay

The results of *in-vitro* antioxidant activity by the ABTS method shows that the screened compound **1** was found to be exhibiting similar activity that of standard, with IC_{50} values of 39.09 µM. SAR studies of ABTS assay was revealed the following results.

Presence of hydroxyl groups on the phenyl ring of both heterocyclic moieties exhibited good radical scavenging ability. The presence of an oxygen atom at the 2nd position of dihydropyrimidinone ring has improved the antioxidant effect. The percentage of inhibition values are given in **Table. XI** and illustrated in **Fig. 11**.

Table XI - The ABTS radical scavenging activity of the synthesized compound **1**

Antioxidant effect of compound 1		
Concentration (µg/mL)	**% Inhibition**	
	1	**Standard**
20	27.15 ± 0.25	28.85 ± 0.72
40	45.44 ± 0.62	47.09 ± 0.27
60	60.39 ± 0.01	67.64 ± 0.57
80	86.17 ± 0.22	83.07 ± 0.80
100	110.13 ± 0.06	108.05 ± 0.70
IC_{50} (µM)	39.09	39.69

Each value is expressed as a percentage of activity mean ± standard deviation (n = 3)

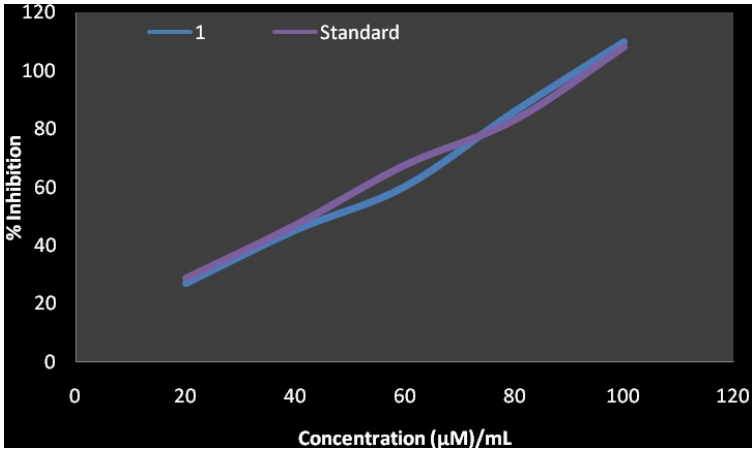

Fig. 11. *In vitro* antioxidant activity by ABTS method of compound **1**

4. CONCLUSIONS

In this work, the novel Dihydropyrimidinone **1** was synthesized and characterized by FT-IR, ^{1}H & ^{13}C-NMR, LC-Mass, UV-Vis, and Fluorescence spectral analysis. The infrared spectrum is simulated using a 6-31G (d, p) base collection using the B3LYP techniques. In order to classify electrophilic and nucleophilic sites in the molecule as well as the possible reaction direction for the synthesized product, Mulliken Charge and Molecular electrostatic potential surface analysis were exploited. Based on the first hyperpolarizability, we infer that a non-linear optical reaction will be given by the investigated molecule and can be used as a non-linear optical substance. In addition, molecular docking is done to clarify the reaction of Dihydropyrimidinone 1 to MCF-7. The anticancer efficacy of the measured novel compound against the MCF-7 cell line by the in-vitro anticancer exploration was shown. The present work details the broad spectrum of antioxidant activity in comparison with a standard. The effect of the title compound on other biological activities such as antitumor, anti-HIV, antimalarial, antihypertensive, etc., which can broaden the therapeutic utility for the compound synthesized, will be a part of future study.

5. REFERENCES

[1] Elkanzi, N. A. A, Heterocyclic Letters, 2013; 3: 247-268.
[2] Barthakur M. G., Borthakur M., Devi, P.,Saikia C. J., Saikia A., Bora U., Chetia A., Boruah R. C., Syn. lett, 2007; 223-226.
[3] Karpov A.S., Müller T. J. J., Synthesis, 2003; 2815-2826.
[4] Movassaghi M., Hill M. D., J. Am. Chem. Soc., 2006; 128: 14254-14255.
[5] Ferrini, F. Ponticelli, M. Taddei, Org. Lett., 2007; 9: 69-72.
[6] Choy N., Blanco B., Wen J., Krishan A., Russel K. C., Org. Lett., 2000; 2: 3761-3764.
[7] Kenner G W and Todd A, "Heterocyclic Compounds" Ed. R C Elderfield, Wiley, New York, 1957; 6.
[8] Brown D J, "The Chemistry of Heterocyclic Compounds" Ed. A. Weissberger, Interscience, New York, 1962; 16.

[9] T.L. Lemke, D.A. Williams, V.F. Roche, S.W. Zito, Wolters kluwer (INDIA), New Delhi, 2008, 6th edn., 117-120
[10] Williams RR, Cline JK. Synthesis of vitamin B1. J Am Chem Soc 1936;58:1504–5.
[11] Reidlinger C, Dworczak R, Fabian WMF, Junek H. Structure– color correlations of penta- and heptamethines: syntheses with nitriles XCIV. Dyes Pigm 1994;24:185–204.
[12] Shaquiquzzaman M, Khan SA, Amir M, Alam MM. Synthesis, anticonvulsant and neurotoxicity evaluation of some new pyrimidine-5-carbonitrile derivatives. Saudi Pharm J 2012;20:149–54.
[13] Prachayasittikul S, Worachartcheewan A, Nantasenamat C, Chinworrungsee M, Sornsongkhram N, Ruchirawat S, et al. Synthesis and structure–activity relationship of 2-thiopyrimidine-4-one analogs as antimicrobial and anticancer agents. Eur J Med Chem 2011;46:738–42.
[14] Brown DJ, Rees CW. Comprehensive heterocyclic Chemistry. 1st ed. Oxford: Pergamon press; 1984.
[15] 7 Zohdi HF, Rateb NM, Elnagdy SM. Green synthesis and antimicrobial evaluation of some new trifluoromethyl-substituted hexahydropyrimidines by grinding. Eur J Med Chem 2011;46:5636–40.
[16] Rahaman SKA, RajendraPasad Y, Kumar P, Kumar B. Synthesis and anti-histaminic activity of some novel pyrimidines. Saudi Pharm J 2009;17:255–8.
[17] Brown DJ, Evans RF. The chemistry of heterocyclic compounds, Vol. 52. New Jersey: John Wiley & Sons Inc.; 1985.
[18] Pasha MA, Ramchandra SM, Jayashankara VP. One pot synthesis of 3,4-dihydropyrimidine 2(1H)-ones/-thiones catalyzed by zinc chloride: an improved procedure for the Biginelli reaction using microwave under solvent free condition. Indian J Chem 2005;44B:823–6.
[19] Kappe CO. Biologically active dihydropyrimidones of the biginelli type- a literature survey. Eur J Med Chem 2000;35:1043–52.
[20] Patil AD, Kumar NV, Kokke WC, Mark FB, Alan JF, Charles DB. Novel alkaloids from the Sponge Batzella sp.: inhibitors of HIV gp120-human CD4 binding. J Org Chem 1995;60:1182–8.